Metallophysics and Advanced Technologies
Металофіз. новітні технол.
Metallofiz. Noveishie Tekhnol.
2022, vol. 44, No. 1, pp. 111–126
https://doi.org/10.15407/mfint.44.01.0111
Reprints available directly from the publisher

PACS numbers: 61.46.-w, 62.20.Qp, 81.05.Ni, 81.40.Pq, 81.65.Kn, 82.45.Bb

Investigation of Mechanical, Wear, and Corrosion Properties of Al–BN–SiC–RHA Hybrid Composites Synthesized Through Powder Metallurgy Process

G. R. Raghav, D. Muthu Krishnan*, K. J. Nagarajan*,
Vidya Chandran, R. Suraj, R. Sujith, S. Dhanesh, and M. S. Anoop

SCMS School of Engineering and Technology,
Vidya Nagar, Palissery, Karukutty, Ernakulam, 683582 Kerala, India
**K.L.N. College of Engineering, Department of Mechanical Engineering,*
630612 Pottapalayam, Sivagangai District, Tamil Nadu, India

Present study explores the effect of Rice Husk Ash (RHA) reinforcements in mechanically alloyed Al–BN–SiC hybrid composites through experimental characterization. The physical, tribological and corrosion resistance properties of Al–BN–SiC–RHA hybrid composites are studied. In the outset the composite pellets are synthesized using powder metallurgy process. The homogenously amalgamated composite powders are then squeezed together to form multiple green composite pellets each measuring 8 mm in diameter using a hydraulic press at a pressure of 500 MPa. The Al–BN–SiC–RHA hybrid composites are characterized using FE-SEM, EDS, and XRD analysis for facilitating the studies on the microstructural as well as the elemental properties. Microhardness and compressive strength of the Al–5BN–5SiC–5RHA hybrid composites is found to improve by 6 and 13.6% respectively compared to those of Al–5BN–5SiC hybrid composites. The RHA reinforced hybrid composites have also experienced reduction in density and an enhancement in the wear resistance of the composite materials while compared to those for their non-RHA counterparts. The electrochemical corrosion analysis of the Al–5BN–5SiC–5RHA hybrid composites also confirms that the Al–5BN–5SiC–5RHA hybrid composites have better corrosion resistance. It is also evident that the corrosion resistance increases with increase in RHA rein-

Corresponding author: G. R. Raghav
E-mail: raghavmechklnce@gmail.com

Citation: G. R. Raghav, D. Muthu Krishnan, K. J. Nagarajan, Vidya Chandran, R. Suraj, R. Sujith, S. Dhanesh, and M. S. Anoop, Investigation of Mechanical, Wear, and Corrosion Properties of Al–BN–SiC–RHA Hybrid Composites Synthesized Through Powder Metallurgy Process, *Metallofiz. Noveishie Tekhnol.*, **44**, No. 1: 111–126 (2022). DOI: 10.15407/mfint.44.01.0111

forcement. On the whole the present RHA based composite yields promising mechanical properties for possible applications in relevant industries.

Key words: RHA, wear, corrosion, FE-SEM, XRD.

Експериментально досліджено вплив зміцнення золою рисового лушпиння (RHA) на механічно леґовані гібридні композити Al–BN–SiC. Вивчено фізичні, трибологічні та корозійні властивості гібридних композитів Al–BN–SiC–RHA. Спочатку композитні гранули синтезували методом порошкової металургії. Потім за допомогою гідравлічного пресу під тиском 500 МПа гомогенно амальгамовані композитні порошки стискали для утворення кількох композитних зелених гранул, кожна розміром 8 мм у діаметрі. Мікроструктуру та властивості гібридних композитів Al–BN–SiC–RHA проаналізовано з використанням FE–SEM (польової емісійної сканувальної електронної мікроскопії), EDS (енергодисперсійної спектроскопії) та XRD (рентґенівської дифракції). Виявлено, що мікротвердість і міцність на стиск гібридних композитів Al–5BN–5SiC–5RHA покращуються на 6 та 13,6% відповідно, порівняно з мікротвердістю гібридних композитів Al–5BN–5Si. Гібридні композити, зміцнені RHA, також мають знижену густину та підвищену зносостійкість порівняно з їхніми аналогами без зміцнення золою рисового лушпиння. Електрохемічний аналіз корозії гібридних композитів Al–5BN–5SiC–5RHA підтверджує, що вони мають кращу корозійну стійкість. Також очевидно, що корозійна стійкість збільшується зі збільшенням зміцнення золою рисового лушпиння. Даний композит на основі RHA має покращені механічні характеристики і може бути застосований у відповідних галузях промисловості.

Ключові слова: зола рисового лушпиння, зносостійкість, корозія, польова емісійна сканувальна електронна мікроскопія, рентґенівська дифракція.

(Received April 12, 2021; in final version, October 10, 2021)

1. INTRODUCTION

Owing to the increase in demand for materials with low density, high strength, better thermal properties with enhanced toughness in the recent past, aluminium (Al) and its alloys are becoming more widely utilized materials [1–6]. The Al based alloys also possess noteworthy tribological and corrosion resistance properties. These alloys are most widely used in automotive, marine and aerospace industries due to the afore mentioned properties. Despite their wide spread use the high cost incurred due to the addition of expensive metal reinforcements such as Cu, W, Ti, Ni and Zr *etc*. keeps their potential undermined [7–11]. The addition of bio-degradable and eco-friendly reinforcements either partially or fully not only reduces the incorporation of hazardous metals but also reduces the production cost of the composite materials. Research has reported considerable works based on eco-friendly materials

such as fly ash, Ground Nut Shell Ash (GNSA) and Rice Husk Ash (RHA) and had also reported the addition of these bio degradable materials leading to positive impact on mechanical, wear and corrosion resistance properties of the composite materials [12, 13].Since a substantial amount of RHA is emerges as an agricultural bi-product wastes, its incorporation not only reduces the cost of production of Al composites but also plays a major role in mitigating environmental contamination. RHA is naturally rich in SiO_2 and TiO_2 which makes it suitable for consideration for potential reinforcements in ceramics due to its good mechanical and also chemical resistant properties [14, 15]. The ceramic particles such as Al_2O_3, ZnO, SiC, B_4C, BN and TiC are the materials which are explored earlier owing to their exceptional mechanical, electrical properties and also because of their availability [16–18]. Further it has also been reported that BN and SiC ceramic particles possesses excellent mechanical and corrosion resistant properties compared to other ceramic particles [8, 19–25].

Few methods such as Powder Metallurgy (PM) [5], stir casting method [8], thermal spraying and physical vapour deposition [9–11] have been developed to fabricate Metal Matrix Composites (MMCs) among which the most widely used method in producing nanocomposites is the PM method. The method entails mixing and compressing powders into a pellet based on the die shape and then sintering process is carried out to further strengthen the composite pellets [13]. Manufacturing nanocomposites through PM route has many advantages over other methods. The main advantage of the PM process is the ability to uniformly amalgamate the materials without any agglomeration. The porosity of the composites can be also controlled by using the PM process. Hence, this method has received much attention compared to other methods [13].

Even though there are few studies based on RHA reinforcements in Al matrix, the effect of RHA reinforcements in Al–BN–SiC hybrid composites is uncharted. Hence, in this study, Al–5BN–5SiC–RHA hybrid nanocomposites with different volumes (5, 10 and 15%) of RHA reinforcing nanoparticles are produced using the PM method at pressure of 500 MPa. The green compacts are sintered in the presence of argon gas at 450°C for 2 hours.

The aim of this work is to study the effect of RHA reinforcement on Al–5BN–5SiC–RHA hybrid nanocomposites and also the effects of different compressive pressure on the mechanical, tribological, and corrosion resistant properties of Al–BN–SiC–RHA hybrid nanocomposites. The hybrid composites are characterized using Scanning Electron Microscopy (SEM), Energy Dispersive Spectrum (EDS) and X-ray Diffraction (XRD) analyses so as to validate microstructure and elements present in the hybrid composites.

2. MATERIALS AND METHODS

2.1. Materials

The materials (Al, BN, SiC) used in the experimental part of this research work are procured from Sigma Aldrich, India. All the powders used in this study are micron in size with research grade quality of 99.5% purity.

2.2. Preparation of RHA

Preparation of RHA marks the beginning of this study. The rice husk is desiccated using sunlight for about two weeks and then placed in a ceramic crucible and subjected to a heat treatment at 700°C in a muffle furnace converting rice husk into ash.

2.3. Preparation of Composite Materials

The Al–5BN–5SiC–RHA hybrid nanocomposites are blended using high energy ball milling process. The base metal (Al) and the reinforcements (5BN, 5SiC) and RHA added in different proportions 1.5, 3, and 5% are measured and fed into the high energy ball mill (Fritsch pulverisette, Germany) and the milling process has been carried out for three hours. To avoid unwanted reaction and overheating of composite powders a dwell period of 15 min/hour is maintained. The blended composite powder is compacted into cylindrical pellets of 8 mm diameter and 40 mm height at a pressure of 500 MPa using a hydraulic press. The hardened composite pellets have thus been obtained after sintering the green compacts at 450°C for about 2 hours in the presence of argon gas.

2.4. Characterization of Composite Materials

FE-SEM, EDS and XRD analyses have been carried out for the characterization of Al–5BN–5SiC–RHA hybrid nanocomposites for studying the morphological arrangements as well as the composition of the composite.

2.5. Density and Microhardness

The densities of the Al–5BN–5SiC–RHA hybrid nanocomposites hybrid composites have been studied using Archimedes' principle as per the ASTM: B962-13 standard. The microhardness test has been performed as per the ASTM E384 standards at five different locations of the composite pellets maintaining a uniform loading condition (1 kgf) and dwell time (10 s).

2.6. Compressive Strength

The determination of compressive strength of the Al–5BN–5SiC–RHA hybrid nanocomposites has been performed using a Universal Testing Machine (UTM) operated at a rate of 5 mm/min at room temperature. The compressive strength and also the percentage deformation of the composite materials have been estimated.

2.7. Wear Analysis

The DUCOM (Bangalore, India) pin on disc wear testing machine has been employed here to research the tribological performance of Al–5BN–5SiC–RHA hybrid nanocomposites as per the ASTM G99-05 standard. A steel rotating circular disc of hardness 65 *HRC* and grade EN32 has been used to mate the surfaces over which the composite pellets are made to slide. An acetone based cleaning of Al–5BN–5SiC–RHA hybrid nanocomposites pellets and the EN32 rotating disc has been ensured prior to the experiment. The weight loss of the composites incurred during sliding wear test has been recorded using a digital weighing machine with a resolution of 0.001 mg. The wear test has been reapeated for a few applied loads (10, 20, and 30 N). The sliding distances have been varied in the range1000–2000 m and sliding speeds 1, 1.5, and 2 m/s, respectively [26–28].

2.8. Electrochemical Corrosion Analysis

In the outset of the corrosion analysis, the RHA based composite samples under consideration have been surface prepared by polishing using abrasive paper of grid sizes 800 and 600 micron and then rinsed with double distilled water. The three electrode electrochemical workstation (Bio-Logic) is made use of hereto study the corrosion performance of the Al–5BN–5SiC–RHA hybrid nanocomposites. A thin platinum wire Ag/AgCl and the Al–5BN–5SiC–RHA hybrid nanocomposites have been considered as counter, reference and working electrodes, respectively. The experiments have been carried out in 5% NaCl electrolyte under room temperature. A scan rate of 1 mV/s is maintained throughout the experiment. The Electrochemical Impedance Spectroscopy (EIS) test for the Al–5BN–5SiC–RHA hybrid nanocomposites are accomplished at the range of 100 kHz to 100 MHz and at the voltage of 5 mV [25, 29, 30].

3. RESULTS AND DISCUSSION

3.1. Characterization of Al–5BN–5SiC–RHA Hybrid Composites

The FE-SEM morphological analysis of the Al matrix and other rein-

forcements such as BN, SiC, RHA and Al–5BN–5SiC–RHA hybrid composites after ball milling are shown in Fig. 1, *a* through *f*).

The FE-SEM micrograph of Al powder is presented in Fig. 1, *a*. The average particle size is approximately 10–20 μm and they exhibit a spherical morphology. Figure 1, *b* represents the FE-SEM micrograph of BN with an average particle size of 2 μm and the particles exhibit flake like structures and are found to be agglomerated. From Figure 1, *c* it can be stated that the average particle size of SiC is approximately 10–30 μm and has crystal like structure. Figure 1, *d* corresponds to the FE-SEM image of RHA which has an average particle size of 50 μm. The FE-SEM image of Al–5BN–5SiC–RHA hybrid composites after ball milling process is shown in Fig. 1, *e*. It is evident that there is uniform amalgamation of Al matrix with BN, SiC and RHA reinforcements. The high magnification FE-SEM images of Al–5BN–5SiC–5RHA hybrid composite is shown in Fig. 1, *f*. It can be seen that there are few pores in the surface of composite pellet. It is also evident that the RHA particles are homogenously mixed and this helped in reducing the porosity of the composites. Figure 2, *a* reveals the EDS spectra of RHA particles which confirm the presence of oxides such as Al_2O_3 and SiO_2 and also the presence of Ca, Cl, Na and K in considerable amount. Figure 2, *b* characterizes the EDS spectra of Al–5BN–5SiC–RHA hybrid composites.

The XRD spectra of RHA particles are shown in Fig. 3. It can be not-

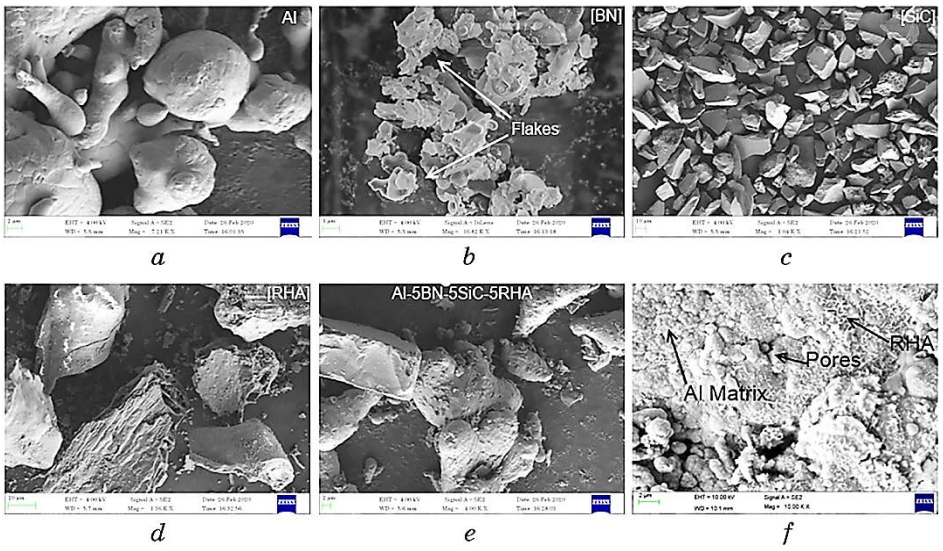

Fig. 1. FE-SEM characterization of Al (*a*), BN (*b*), SiC (*c*), RHA (*d*), Al–5BN–5SiC–5RHA hybrid composites after ball milling (*e*), high magnification FE-SEM image of Al–5BN–5SiC–5 RHA hybrid composite pellet (*f*).

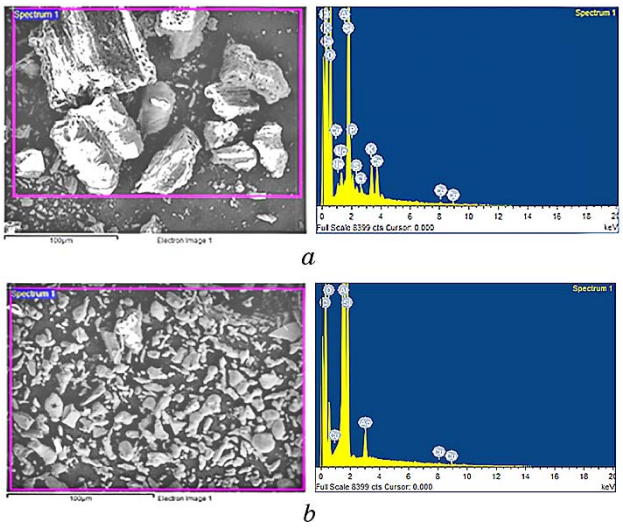

Fig. 2. EDS images of RHA (*a*), Al–5BN–5SiC–RHA hybrid composites (*b*).

ed that the RHA particles has characterized peaks at 2θ = 27° and 46° which correspond to SiO_2.

Hence it can be confirmed that RHA is composed of SiO_2. From the XRD of RHA it can be confirmed that the RHA particles are irregular in size ranging from micro to nanoscale due to the broadening of peak at 25° and thin peaks elsewhere. Figure 4 shows the XRD spectra of Al–5BN–5SiC–5 RHA hybrid composites after ball milling. From the XRD analysis it is evident that there is a presence of all constituents and are clearly visible in XRD spectra. Further, there is no formation

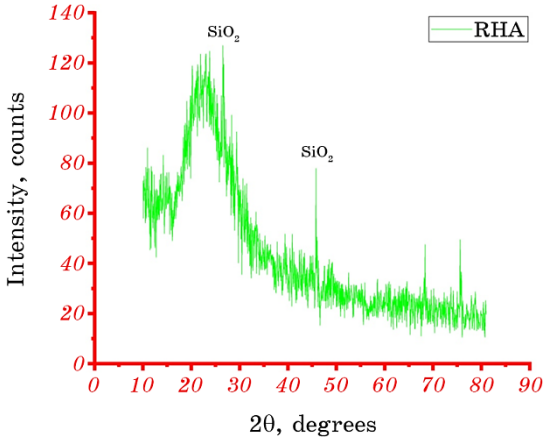

Fig. 3. XRD pattern of RHA particles.

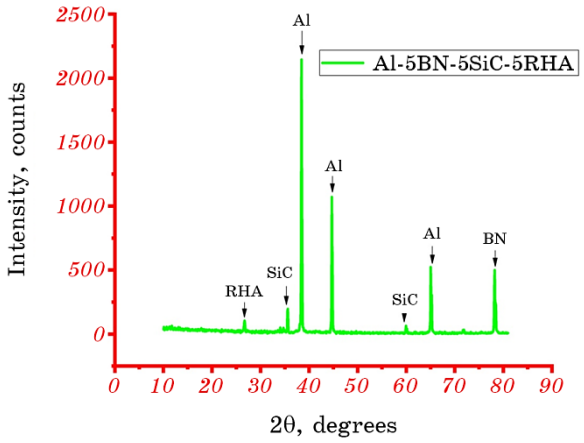

Fig. 4. XRD pattern of Al–5BN–5SiC–5RHA hybrid composites.

of intermetallic compounds which confirms the absence of any chemical reaction between Al matrix and BN, SiC and RHA reinforcements. The characteristic peaks at the $2\theta = 39.25°$, 45° and 65° confirms the presence of Al particles. The presence of BN can be confirmed based on the peak at $2\theta = 78°$. The presence of SiC and RHA can be confirmed from the peaks at 36°, 60°, and 27°, respectively.

3.2. Characterization of Mechanical Properties

The relation between compressive strength and percentage of deformation is shown in Fig. 5. The compressive strength of the Al–

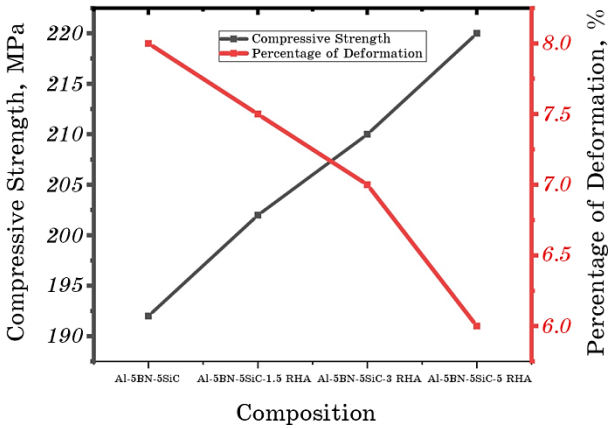

Fig. 5. Graphical representation of percentage of deformation and compressive strength of Al–5BN–5SiC–RHA hybrid composites.

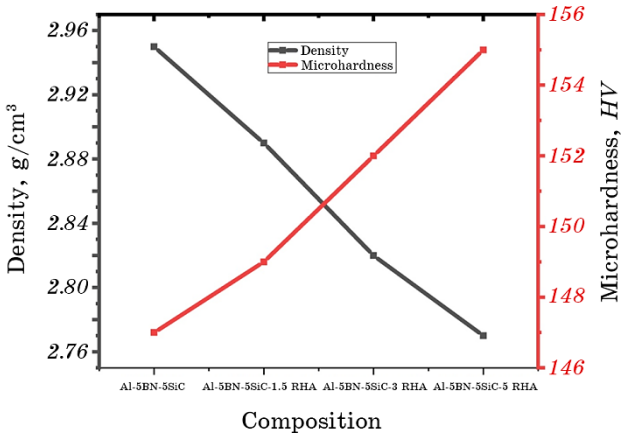

Fig. 6. Graphical representations of density and microhardness of Al–5BN–5SiC–RHA hybrid composites.

5BN–5SiC hybrid composite is found to be190 MPa. The results show that the RHA reinforcements has positive effect on improvingthe compressive strength of Al–5BN–5SiC hybrid composites. The compressive strength of Al–5BN–5SiC–1.5RHA hybrid compositehas improved slightly to 202 MPa which further increased to 220 MPa for Al–5BN–5SiC–5 RHA hybrid composite. The percentage deformation of the Al–5BN–5SiC hybrid composite is around 8% whereas the percentage of deformation of Al–5BN–5SiC–5RHA hybrid composites are reduced to 6% , which is attributed due to the unifrom dispersion of RHA reinforcement which has the presence of SiO_2 particles. The effect of RHA particles on the density and microhardness of the Al–5BN–5SiC hybrid composites is shown in Fig. 6. From the graph it is observed that the density of the composite materials decreases with reinforcement of less denser RHA particles.

The Al–5BN–5SiC hybrid composites has achieved a density of 2.95 g/cm^3 compared to that of Al–5BN–5SiC–5 RHA hybrid composites which is found to be around 2.77 g/cm^3. The microhardness of the Al–5BN–5SiC–5 RHA hybrid composites is found to be superior at 155 HV compared to that of Al–5BN–5SiC hybrid composites which is 147 HV. The increase in microhardness is due to the presence of SiO_2 particles which is the prominent element in the RHA.

3.3. Wear Analysis

Figure 7 displays the average wear rate of Al–5BN–5SiC–RHA hybrid composites under diverse sliding conditions such as sliding speed, sliding distance and load. The wear rate at different applied loads and constant sliding speed and sliding distance of 1.5 m/s and 1500 m respec-

tively displayed in the Fig. 7, *a*. From the experimental results it can be understood that the increase in load has increased the wear rate of the composites and further Al–5BN–5SiC–5RHA hybrid composites has lesser wear rate compared to Al–5BN–5SiC hybrid composites.

The presence of RHA particles has resulted in reduction of wear of the composites due to the relatively hard nature of the SiO_2 which is the prominent element in the RHA. The increase in wear rate with respective to load is also due to the increase in contact area between the specimen and the EN32 rotating disc. From Fig. 7, *b* it is evident that with the raise in sliding speed, the specimens have been subjected to more wear rate owing to the high pressure between the mating surfaces which increases the temperature at contact surfaces which leads to the deformation of the composite specimens. Figure 7, *c* represents the wear rate of composite specimens at varying sliding distance. The wear rate of the Al–5BN–5SiC hybrid composites has decreased considerably with the RHA reinforcement. However the wear of the composite specimens increases with the sliding distance which is due the increase in contact period of the mating EN32 and composite pellets.

The coefficient of friction of the Al–5BN–5SiC–RHA hybrid composites at diverse operating conditions such as applied load, slid-

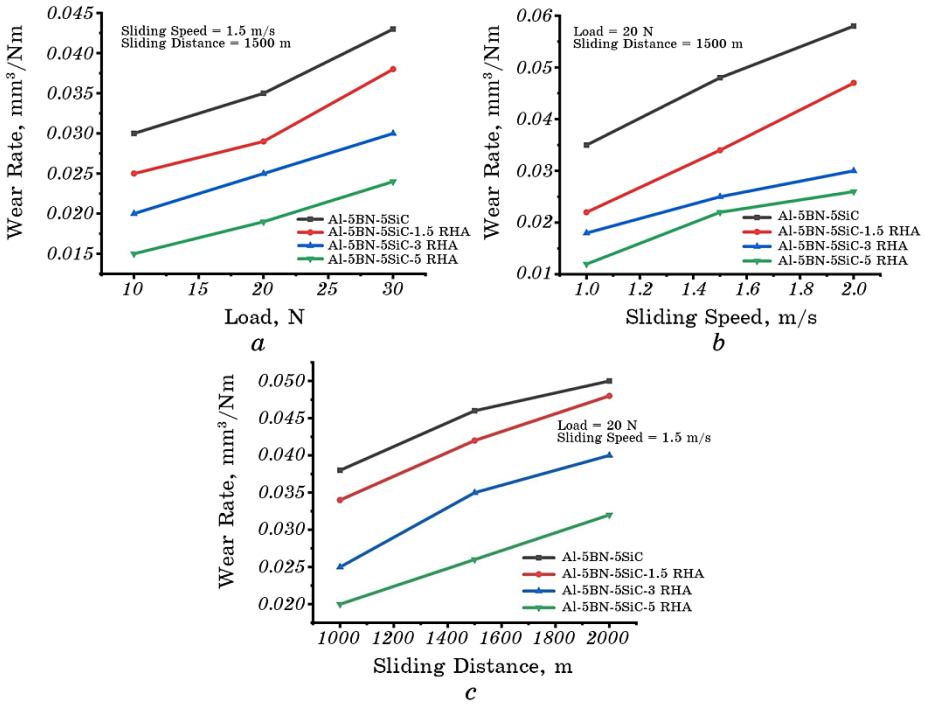

Fig. 7. Wear rate of Al–5BN–5SiC–RHA hybrid composites.

ing speed and sliding distance is shown in Fig. 8. From Figure 8 it is obvious that the coefficient of friction of the Al–5BN–5SiC–RHA hybrid composites has improved with addition of RHA particle reinforcement. The coefficient of friction of Al–5BN–5SiC–5RHA hybrid composites has improved 20% compared to Al–5BN–5SiC hybrid composites under all sliding conditions. This improvement in the coefficient of friction is due to the presence of RHA (SiO_2) particles in the composite materials.

Figure 9, *a* represents the surface micrograph of Al–5BN–5SiC–5RHA hybrid composite pellet after the wear testat the magnifiaction of 350 times.

It can be noted that the specimens sufer a absrasive wear initially and followed by adhesive wear which is due to the sofening of the composite materials as a result of high temperature caused due to mating of contacting surfaces.

Figure 10, *b* shows the high magnifigation (×1.5) SEM image of the Al–5BN–5SiC–5RHA hybrid composite pellet after the wear test. From the image it is clear that there is adhesive wear followed by abrasive wear and there is evidence of material removal due to plastic deformation. Figures 10, *c*, *d* represent the high resolution (×10) FE-

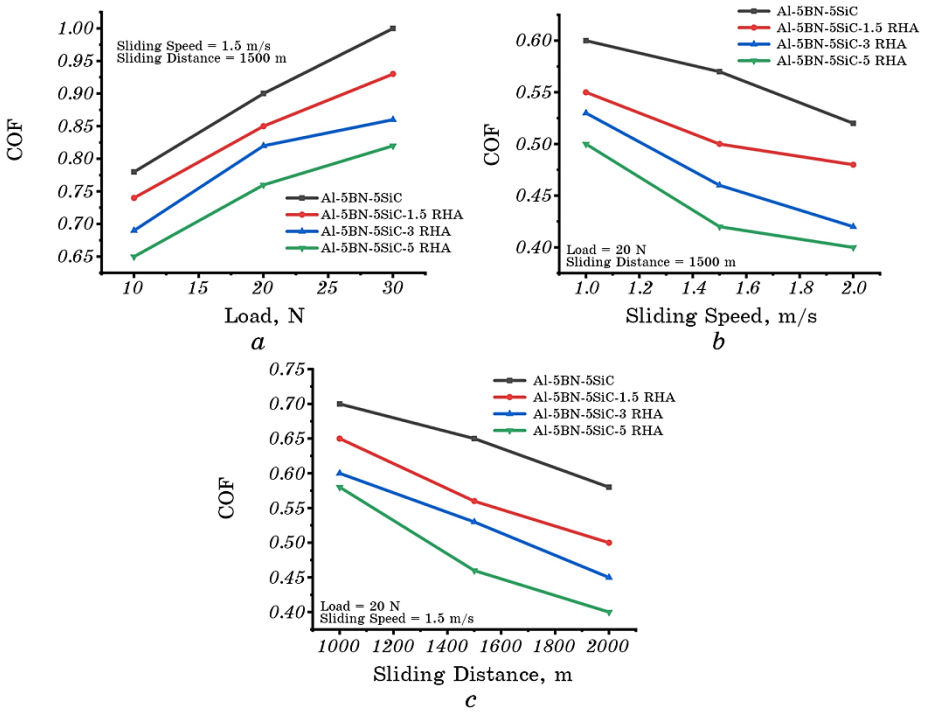

Fig. 8. Coefficient of friction of Al–5BN–5SiC–RHA hybrid composites.

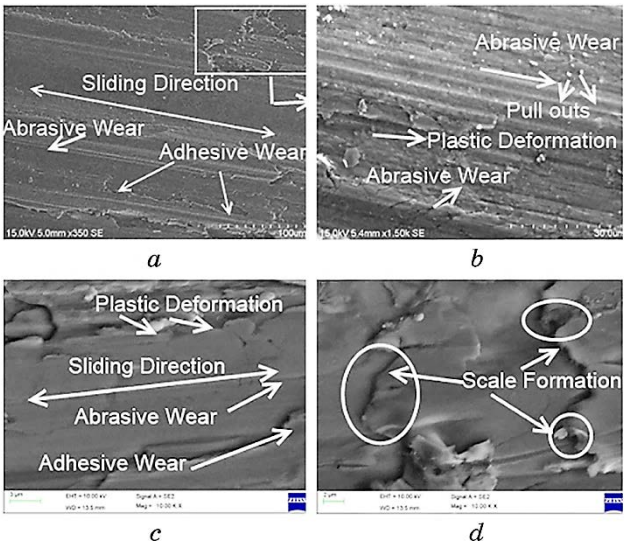

Fig. 9. Surface of Al–5BN–5SiC–RHA hybrid composites after wear test (*a*); ×1.5 magnification of Al–5BN–5SiC–RHA hybrid composites (*b*); ×10 magnification FE-SEM of Al–5BN–5SiC–RHA hybrid composites (*c*, *d*).

SEM images of Al–5BN–5SiC–5RHA hybrid composite pellet after the wear test.

It can be observed that there is ploughing like effect such as formation of scraches and grooves confirms the hard and ductile nature of thehybrid composites and also confirms that the major wear mechanism is abrasive wear and scaling like material removal which leads to adhesive wear followed by plastic deformation.

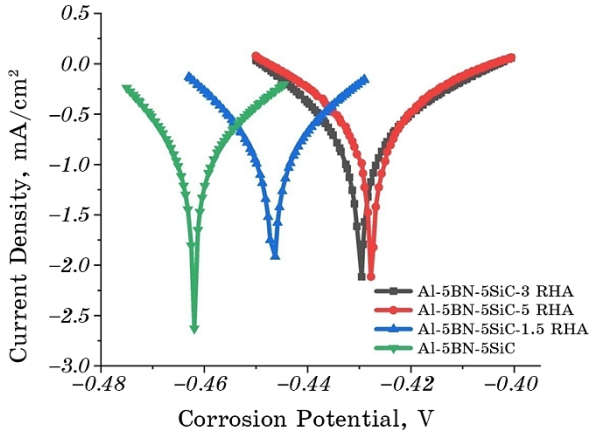

Fig. 10. Tafel plot of Al–5BN–5SiC–RHA hybrid composites.

3.4. Corrosion Analysis

The Al–5BN–5SiC–RHA hybrid composites are immersed in NaCl solution for 2 hours for stabilizing the open circuit potential. The potentiodynamic polarization curves of the tested Al–5BN–5SiC–RHA hybrid composites are shown in Fig. 10. The Tafel extrapolation method (Table 1) has been utilized to calculate corrosion current (I_{corr}) and corrosion potential (E_{corr}), respectively. The corrosion current densities of the various tested samples range from 1 mA/cm^2 to 0.7 mA/cm^2. The corrosion current density of Al–5BN–5SiC–5RHA hybrid composite is 0.7 mA/cm^2 which is lower compared to that of other combinations. The Al–5BN–5Si hybrid composites yielded a corrosion current density of 1 mA/cm^2. Hence based on the corrosion current density we can conclude that Al–5BN–5SiC–5RHA hybrid composites have better corrosion resistance attributed to the presence of RHA (SiO_2) which resists the corrosion.

The corrosion potential (E_{corr}) of the Al–5BN–5SiC–5RHA hybrid composites is found to be around –0.4299 V which is far better than other combinations such as Al–5BN–5SiC–1.5RHA (–0.447 V) and Al–5BN–5SiC (–0.468 V) hybrid composites which confirms the improvement in the corrosion resistance. EIS spectroscopic analysis is also used to study the corrosion resistance nature of Al–5BN–5SiC–RHA hybrid composites. The two dissimilar semicircles are characterized as an outcome of electron transfer which takes place within the Al–5BN–5SiC–RHA hybrid composites and diffusion between the Al–5BN–5SiC–RHA hybrid composites and NaCl solution which corresponds to larger and smaller arc respectively as shown in Fig. 11 [30–32]. In this study it is observed that there is no occurrence of perfect capacitance behaviour, hence a constant phase element (CPE) is introduced in the equivalent circuit [33, 34].

The Table 2 represents the various EIS parameters such as resistance and CPE values of the Al–5BN–5SiC–RHA hybrid composites. It is indeed noticeable that the charge transfer resistance R_{ct1} of the Al–5BN–5SiC–5RHA hybrid composites (R_{ct1} = 22.50 Ω·cm^2) has improved slightly than that of pure Al–5BN–5Si hybrid composites (R_{ct1} = 14 Ω·cm^2) which point out that there is improvement in corro-

TABLE 1. Tafel extrapolation results of Al–5BN–5SiC–RHA hybrid composites.

Number	Specimen	E_{corr}, V	I_{corr}, mA/cm^2
1	Al–5BN–5SiC	–0.468 ± 0.101	1 ± 0.023
2	Al–5BN–5SiC–1.5RHA	–0.447 ± 0.087	0.9 ± 0.012
3	Al–5BN–5SiC–3RHA	–0.431 ± 0.053	0.72 ± 0.011
4	Al–5BN–5SiC–5RHA	–0.429 ± 0.021	0.7 ± 0.006

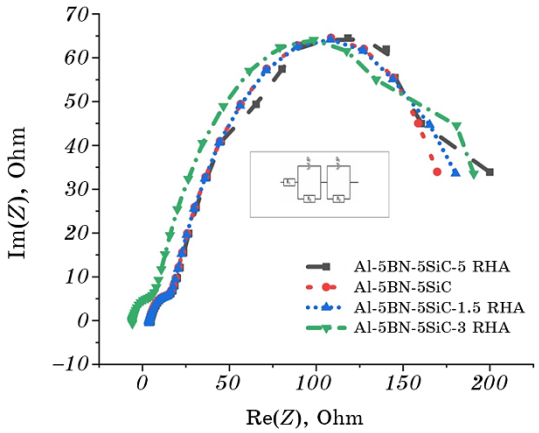

Fig. 11. EIS plot of Al–5BN–5SiC–RHA hybrid composites.

TABLE 2. EIS data obtained by fitting equivalent circuit model (standard deviation σ).

No.	Specimen	R_s, Ω·cm^2	Q_2, F·cm^{-2}	C_{dl1}, F·cm^{-2}	R_{ct1}, Ω·cm^2	Q_3, F·cm^{-2}	C_{dl2}, F·cm^{-2}	R_{ct2}, Ω·cm^2
1	Al–5BN–5SiC	–0.154 ± ± 0.220	0.0952	0.0984	14 ± ± 0.15	0.1221	0.0784	170.32 ± ± 6.32
2	Al–5BN–5SiC–1.5RHA	3.245 ± ± 0.125	0.0531	0.0723	22.21 ± ± 0.22	0.1200	0.0634	175.20 ± ± 5.22
3	Al–5BN–5SiC–3RHA	3.254 ± ± 0.153	0.0522	0.0701	22.34 ± ± 0.21	0.1185	0.0612	191.17 ± ± 4.34
4	Al–5BN–5SiC–5RHA	3.352 ± ± 0.212	0.0508	0.0689	22.50 ± ± 0.23	0.1178	0.0584	201.14 ± ± 4.50

sion resistance of Al–5BN–5SiC–5RHA hybrid composites.

The addition of RHA particles has resulted in reduction of charge transfer capacitance of the Al–5BN–5SiC–RHA hybrid composites. The true capacitance also shows that the Al–5BN–5SiC–5RHA hybrid composites ($C = 0.0689$ F·cm^{-2}) have lesser capacitance value compared to Al–5BN–5Si hybrid composites ($C = 0.0984$ F·cm^{-2}).

4. CONCLUSIONS

The powder metallurgy methods and processes have been employed here to synthesize the Al–5BN–5SiC–RHA hybrid composites. The mechanical, wear and corrosion resistance of the Al–5BN–5SiC–RHA hybrid composites are here with examined and reported.

The addition of RHA particles has improved the microhardnessof

the Al–5BN–5SiC–5RHA hybrid composites (155 HV) notably compared to that of Al–5BN–5SiC hybrid composites (147 HV).

The RHA particle reinforcement has improved the compression strength of the Al–5BN–5SiC–5RHA hybrid composites (220 MPa) by 13.6% when compared to Al–5BN-5SiC hybrid composites (190 MPa).

In contrast the density of the Al–5BN–5SiC–RHA–5RHA hybrid composites (2.77 g/cm^3) has decreased nearly 6% due to the RHA reinforcement.

The wear rate and COF values shows that Al–5BN–5SiC–5RHA hybrid composites have enhanced wear resistance properties.

The Tafel plot analysis shows that the Al–5BN–5SiC–5RHA hybrid composites have higher corrosion resistance.

The EIS corrosion analysis also indicates that the Al–5BN–5SiC–5RHA hybrid composite has enhanced corrosion resistance.

From the conclusions drawn above, it can be accomplished that the addition of RHA reinforcements has reduced the density of the composite materials on the other hand has also enhanced the other mechanical properties such as wear and corrosion resistance of the Al–5BN–5SiC–5RHA hybrid composites. On the whole study provides very useful information on the characterization and material properties of a potential novel composite material.

ACKNOWLEDGEMENTS

The authors would like to thank the Management and Principal of K.L.N College of Engineering, Madurai, India; MEPCO Schlenk Engineering College, Sivakasi, India, and Gandhigram University, Dindigul, India for their constant encouragement, support and providing all the essential facilities for completing this research work.

REFERENCES

1. H. Guoxin, X. Zhengxia, L. Jianju, and L. Yanhong, *Surf. Coat. Technol.*, **203**: 3392 (2009).
2. K. N. P. Prasad and M. Ramachandra, *Mater. Today Proceedings*, **5**, Iss. 1, Part 3: 2844 (2018).
3. A. V. Pshyk, L. E. Coy, L. Yate, K. Załeski, G. Nowaczyk, A. D. Pogrebnjak, and S. Jurga, *Mater. Des.*, **94**: 230 (2016).
4. A. Pal, S. Poria, G. Sutradhar, and P. Sahoo, *Mater. Res. Express*, **5**: 036521 (2018).
5. H. Sharifi, K. Ostovan, M. Tayebi, and A. Rajaee, *Tribol. Int.*, **116**: 244 (2017).
6. Y. Gao, F. Qiu, S. Shu, L. Wang, and F. Chang, *Arch. Civ. Mech. Eng.*, **18**: 179 (2017).
7. T. S. Kumar, R. Subramanian, S. Shalini, and P. C. Angelo, *Forsh. Ingenieurwes.*, **79**: 123 (2015).

8. S. Suresh, N. S. Vinayaga, S. C. Vettivel, N. Selvakumar, and G. R. Jinu, *Mater. Sci. Eng. A*, **612**: 16 (2014).
9. P. V. K. Raju, S. Rajesh, J. B. Rao, and N. R. M. R. Bhargava, *Mater. Today Proc.*, **5**: 885 (2018).
10. K. K. Kishore, S. B. V. Siva, J. B. Rao, and N. R. M. R. Bhargava, *Mater. Today Proc.*, **5**: 3719 (2018).
11. B. P. Dileep, V. Ravikumar, and H. R. Vital, *Mater. Today Proc.*, **5**: 12257 (2018).
12. M. Bilal, N. Shaikh, S. Raja, M. Ahmed, M. Zubair, A. Khan, and M. Ali, *Mater. Res. Express*, **6**, No. 5: 056518 (2019).
13. G. R. Raghav, D. Muthu Krishnan, R. Sundar, R. Ashokkumar, and K. J. Nagarajan, *Eng. Res. Express*, **2**: (2020).
14. R. Hofman, J. G. F. Westheim, I. Pouwel, T. Fransen, and P. J. Gellings, *Surf. Interface Anal.*, **24**: 1 (1996).
15. G. R. Raghav, N. Selvakumar, and K. J. M. R. Thansekhar, **3**: 1105 (2014).
16. Shi-cheng Wei, Bin-shi Xu, Hai-dou Wang, Guo Jin, and Hong Lv, *Surf. Coatings Technol.*, **201**: 5294 (2007).
17. X. Zhao, Y. An, J. Chen, H. Zhou, and B. Yin, *Wear*, **265**: 1642 (2008).
18. L. N. Dyachkova, E. E. Feldshtein, P. A. Vityaz, B. M. Błoch, and L. Ya. Voronetskaya, *J. Frict. Wear*, **39**: 1 (2018).
19. H. A. Jehn, *Surf. Coat. Technol.*, **125**: 212 (2000).
20. R. V. Prasad Kaviti, D. Jeyasimman, G. Parande, M. Gupta, and R. Narayanasamy, *J. Magnes. Alloys*, **6**: 263 (2018).
21. X. Zhang, J. Ma, J. Yang, Q. Bi, and W. Liu, *Wear*, **271**: 881 (2011).
22. P. Narayanasamy, N. Selvakumar, and P. Balasundar, *Mater. Today Proc.*, **5**: 6570 (2018).
23. H. Ge, Q. Song, W. Hu, B. Zhang, Y. Jia, Y. Liu, M. Ma, and R. Liu, *J. Alloys Compd.*, **750**: 96 (2018).
24. W. Xi, H. Wang, J. Li, and C. Shi, *Mater. Sci. Eng. A*, **541**: 166 (2012).
25. S. Gopinath, M. Prince, and G. R. Raghav, *Mater. Res. Express*, **7**: 016582 (2020).
26. G. R. Raghav, A. N. Balaji, D. Muthukrishnan, and V. Sruthi, *Metallofiz. Noveishie Tekhnol.*, **40**, No. 7: 979 (2018).
27. G. R. Raghav, A. N. Balaji, N. Selvakumar, D. Muthukrishnan, and E. Sajith, *Mater. Res. Express*, **6**, No. 11: 1165e4 (2019).
28. G. R. Raghav, A. N. Balaji, D. Muthukrishnan, V. Sruthi, and E. Sajith, *Mater. Res. Express*, **5**: 066523 (2018).
29. D. Muthukrishnan, A. N. Balaji, and G. R. Raghav, *Metallofiz. Noveishie Tekhnol.*, **40**: 397 (2018).
30. S. A. Umoren, Y. Li, and F. H. Wang, *Corros. Sci.*, **53**: 1778 (2011).
31. A. Ehsani, M. G. Mahjani, M. Hosseini, R. Safari, R. Moshrefi, and H. Mohammad Shiri, *J. Colloid Interface Sci.*, **490**: 444 (2017).
32. E. Angelini, S. Grassini, F. Rosalbino, F. Fracassi, and R. D'Agostino, *Prog. Org. Coatings*, **46**: 107 (2003).
33. E. Kowsari, S. Y. Arman, M. H. Shahini, H. Zandi, A. Ehsani, R. Naderi, A. Pourghasemi Hanza, and M. Mehdipour, *Corros. Sci.*, **112**: 73 (2016).
34. M. Hosseini, L. Fotouhi, A. Ehsani, and M. Naseri, *J. Colloid Interface Sci.*, **505**: 213 (2017).